The Analysis on the L-index based Optimal Power Flow Considering Voltage Stability Constraints

HAILUN HUANG, YIGANG KONG
Department of Electrical Engineering
Shanghai Jiaotong University
Minhang District, Shanghai 200240
CHINA
hailunhhl@sjtu.edu.cn, yigangkong@163.com

JIAN ZHANG
Department of Information Technology
Uppsala University
P.O. Box 256, SE-751 05 Uppsala
SWEDEN
zxmc2002@yahoo.com.cn

Abstract: - In the environment of electricity markets, power systems are operated nearer against the voltage stability limit than before. For this reason, this paper presents a novel optimal power flow (OPF) formulation containing voltage stability constraints. By adopting the L index function that can reflect stability margin from the collapse point as voltage stability constraints, this model can obtain the demanded voltage security level by adjusting the upper limits of these constraints. So its optimal solution can satisfy the security and economical demand of power systems simultaneously. At the same time, the primal-dual interior point method (IPM) based on the perturbed Karush-Kuhn- Tucker (KKT) conditions is proposed to solve this problem. Simulation results on five test systems demonstrate the effectiveness of the presented OPF model with voltage stability constraints, and the proposed computation approach has good convergence.

Key-Words: - Optimal power flow; Voltage stability; L index; Primal-dual interior point method

1 Introduction

OPF is a powerful tool for power system analysis [1], and a lot of work has been done to develop effective schemes for its solving and application for many years [2,3]. In the competitive market environment, power systems will have to be operated at higher loading conditions with market influences demanding greater attention to operating cost. This may increase the possibility of voltage instability incidents [4]. So how to consider voltage stability in OPF formulation is a new challenge to us.

Voltage stability is an important aspect of security analyses in power system planning and operation. To measure the severity level of voltage stability problems, a lot of performance indices have been proposed [5]. They could be used on-line or off-line to help operators determine how close the system is to collapse. In general, these indices aim at defining a scalar magnitude that can be monitored as system parameters change, with fast computation speed. They include the sensitivity factors [6-9], second order performance index [10,11], voltage instability proximity index (VIPI) [12-14], singular values and eigenvalues [15-19], and so on.

As to the possibility of including stability constraints into standard OPF formulations, [20] discusses the issue and [21] develops a conceptual framework. Several hybrid OPF formulations incorporating voltage stability constraints are presented in [22,23]. That method puts requirements on evaluating the critical point of voltage stability, so the problem size and computation burden are enhanced. [24] reports an optimal dispatch with voltage stability constraints, using the bifurcation technique to calculate the voltage stability margin. [25] proposes a voltage stability constrained OPF with the modified form of L-index as voltage stability constraints. The modified index may be different from its initial form in indicating voltage stability and affecting the OPF model.

As a result, in our study we use the initial form of L-index to indicate the voltage security and construct a novel OPF formulation that can consider

voltage stability margin of the system. This model has an advantage that there is no necessity to calculate the critical point. Different results are obtained in that the effective range of L-index constraints is not as large as that of the modified form in [25]. Moreover, the perturbed-KKT-condition based primal-dual IPM is applied as the solution approach. It is proved to be efficient by the simulation results.

The paper is organized as follows. In Section 2 the L-index based OPF formulation with voltage stability constraints is presented, and then the computational implementation is introduced. Simulation results are given in Section 4. Section 5 is the conclusion.

2 L-index Based OPF Considering Voltage Stability Constraints

In our study OPF is formulated in the rectangular form. The objective function to be minimized is the fuel cost of thermal plants. So the OPF problem incorporating voltage stability constraints can be formulated as:

$$\text{minimize } f(x)=\sum_{i=1}^{S_G}(a_{0i}+a_{1i}P_{Gi}+a_{2i}P_{Gi}^2) \quad (1)$$

subject to:

(1) Power flow equations:

$$\begin{cases} P_{Gi}=P_{Di}+\sum_{j=1}^{n}(e_i(e_jG_{ij}-f_jB_{ij})+f_i(f_jG_{ij}+e_jB_{ij})) \\ Q_{Ri}=Q_{Di}+\sum_{j=1}^{n}(f_i(e_jG_{ij}-f_jB_{ij})-e_i(f_jG_{ij}+e_jB_{ij})) \end{cases} \quad (2)$$

$$i=1,2,\cdots,n$$

(2) System operational constraints:

$$\begin{cases} \underline{|V_i|}^2\le(e_i^2+f_i^2)\le\overline{|V_i|}^2 & i=1,2,\cdots,n \\ \underline{P}_{Gi}\le P_{Gi}\le\overline{P}_{Gi} & i\in S_G \\ \underline{Q}_{Ri}\le Q_{Ri}\le\overline{Q}_{Ri} & i\in S_R \\ \underline{P}_{ij}\le P_{ij}\le\overline{P}_{ij} & (i,j)\in S_{CL} \\ P_{ij}=(e_i^2+f_i^2-e_ie_j-f_if_j)G_{ij}+(e_if_j-e_jf_i)B_{ij} & \end{cases} \quad (3)$$

(3) Voltage stability constraints:

$$0\le L_i\le\overline{L} \qquad i\in S_L \quad (4)$$

where:

a_{0i}, a_{1i}, a_{2i}	:	fuel cost coefficients of thermal plant i
$G_{ij}+jB_{ij}$	:	transfer admittance between buses i and j
e_i+jf_i	:	real and imaginary part of the volatge V_i at bus i
P_{Gi}, Q_{Ri}	:	dispatchable active and reactive power at bus i
P_{Di}, Q_{Di}	:	active and reactive power demand at bus i
S_G, S_R	:	set of thermal plants and reactive power sources
$\underline{(\bullet)}, \overline{(\bullet)}$	:	lower and upper limits of variables or quantities
(i, j)	:	transmission line connecting bus i and j
S_{CL}	:	set of constrained lines
S_L	:	set of constrained lines
P_{ij}	:	active power of transmission line (i, j)
L_i	:	L index evaluated at load bus i
$\overline{L}$	:	the upper limit of the index acceptable for the system
n	:	the number of total buses

It can be observed that the above OPF formulation is to add a group of voltage stability margin constraints (4) on the basis of the conventional OPF. Thus, the optimal solution of this model can not only minimize the total fuel cost, but also guarantee a certain level of voltage security for the system.

2.1 Voltage Stability Constraints

L index is proposed as a good voltage stability indicator with its value change between zero (no load) and one (voltage collapse) [26]. Moreover, it can be used as a quantitative measure to estimate the voltage stability margin against the operating point. Therefore, we use this index to create the voltage stability constraints in our model.

The index L at the load bus i can be given by

$$L_i = \left| 1 - \frac{\sum_{j \in S_G} F_{ij} V_j}{V_i} \right| \tag{5}$$

where

the voltage V_i is given by

$$V_i = \sum_{i \in S_L} Z_{ij} I_j + \sum_{i \in S_G} F_{ij} V_j \tag{6}$$

Z_{ij} and F_{ij} are respectively the corresponding elements of the sub-matrices Z_{LL} and F_{LG} in the matrix H in the following equation (7).

$$\begin{bmatrix} V_L \\ I_G \end{bmatrix} = H \begin{bmatrix} I_L \\ V_G \end{bmatrix} \tag{7}$$

$$H = \begin{bmatrix} Z_{LL} & F_{LG} \\ K_{GL} & Y_{GG} \end{bmatrix} \tag{8}$$

V_L, I_L: the vector of voltages and currents of the load buses;

V_G, I_G: the vector of voltages and currents of the generator buses;

$Z_{LL}, F_{LG}, K_{GL}, Y_{GG}$: sub-matrices of the hybrid matrix H .

The matrix H can be generated by the partial inversion of the bus admittance matrix, where the voltages at load buses are exchanged against their currents.

L_i could also be calculated by way of the nodal complex power S_i as follows:

$$L_i = \left| \frac{(S_i + S_{icorr})^*}{Y_{ii+} \cdot V_i^2} \right| \tag{9}$$

where

$$S_{icorr} = \left(\sum_{j \in S_L}^{j \neq i} \frac{Z_{ij}^*}{Z_{ii}^*} \cdot \frac{S_j}{V_j} \right) \cdot V_i \tag{10}$$

$$Y_{ii+} = 1 / Z_{ii} \tag{11}$$

* indicates the complex conjugate of the vector, S_{icorr} represents the contributions of the other loads in the system to the index evaluated at the bus i.

The above description tells us that L index will get close to 1.0 when a load bus approaches the steady state voltage stability limit. So if the index evaluated at any bus is less than unity, the system can keep voltage stability.

2.2 The Primal-Dual IPM

The perturbed-KKT-condition based primal-dual IPM proposed in [27] is improved from the initial IPM [28]. As a polynomial-time algorithm, the primal-dual IPM possesses quadratic convergence and has no strict demand on the initial values. Thus it is very efficient in solving the large-scale nonlinear programming (NP) problems [29].

In this section we will explain how to apply this approach to solve the OPF problem with voltage stability constraints.

Here we use the following form of NP problems for better illustration:

$$\begin{aligned} &\min \quad f(x) \\ &s.t. \quad h(x)=0 \\ &\qquad \underline{g} \le g(x) \le \overline{g} \end{aligned} \tag{12}$$

where

$$\begin{aligned} h(x) &= [h_1(x), \cdots, h_m(x)]^T \\ g(x) &= [g_1(x), \cdots, g_r(x)]^T \end{aligned} \tag{13}$$

By introducing slack variable vectors $(l,u) \in R^{(r)}$, system (12) is transformed to:

$$\begin{aligned} &\min \quad f(x) \\ &s.t. \quad h(x)=0 \\ &\qquad g(x)-l-\underline{g}=0, g(x)+u-\overline{g}=0 \\ &\qquad (l,u) \ge 0 \end{aligned} \tag{14}$$

Define a Lagrangian function associated with (14) as:

$$L \equiv f(x) - y^T h(x) - z^T (g(x) - \underline{g} - l) - w^T (g(x) - \overline{g} + u) - \overline{z}^T l - \overline{w}^T u \quad (15)$$

Note that the following relationships hold:

$$\frac{\partial L}{\partial l} = z - \overline{z} = 0, \frac{\partial L}{\partial u} = -w - \overline{w} = 0 \quad (16)$$

where $y \equiv R^m$, $(z, w, \overline{z}, \overline{w}) \in R^{(r)}$ are Lagrangian multipliers.

Then, we can derive the following KKT equations for system (12):

$$\begin{cases} L_x = \nabla f(x) - \nabla h(x) y - \nabla g(x)(z + w) = 0 \\ L_y = h(x) = 0 \\ L_z = g(x) - \underline{g} - l = 0 \\ L_w = g(x) - \overline{g} + u = 0 \\ L_l = LZe - \mu e = 0 \\ L_u = UWe - \mu e = 0 \end{cases} \quad (17)$$

where u is the perturbed factor, $(l, u, z) \geq 0$, $w \leq 0, y \neq 0$, $(L, U, Z, W) \in R^{(r \times r)}$ are all diagonal matrices and $e = [1, \cdots, 1]^T \in R^{(r)}$.

Thus, by applying Newton's method to the perturbed KKT equations, we can obtain the following correction equations:

$$M_{cor} \bullet \begin{bmatrix} \Delta x \\ \Delta y \\ \Delta z \\ \Delta w \\ \Delta l \\ \Delta u \end{bmatrix} = - \begin{bmatrix} L_{x0} \\ L_{y0} \\ L_{z0} \\ L_{w0} \\ L^{\mu}_{l0} \\ L^{\mu}_{u0} \end{bmatrix} \quad (18)$$

where

$$M_{cor} = \begin{bmatrix} F & -\nabla h(x) & -\nabla g(x) & -\nabla g(x) & 0 & 0 \\ \nabla^T h(x) & 0 & 0 & 0 & 0 & 0 \\ \nabla^T g(x) & 0 & 0 & 0 & -I & 0 \\ \nabla^T g(x) & 0 & 0 & 0 & 0 & I \\ 0 & 0 & L & 0 & Z & 0 \\ 0 & 0 & 0 & U & 0 & W \end{bmatrix} \quad (19)$$

$$F = \nabla^2 f(x) - \nabla^2 h(x) y - \nabla^2 g(x)(z + w) \quad (20)$$

$L_{x0}, L_{y0}, L^{\mu}_{l0}, L^{\mu}_{u0}, L_{z0}$ and L_{w0} are the residuals of the perturbed KKT equations; $\nabla^2 h(x)$ and $\nabla^2 g(x)$ are Hessian matrices of $h(x)$ and $g(x)$.

Solve the correction equation (18), and update the primal and dual variables with the following formula:

$$\begin{bmatrix} x \\ l \\ u \end{bmatrix} = \begin{bmatrix} x \\ l \\ u \end{bmatrix} + step_P \begin{bmatrix} \Delta x \\ \Delta l \\ \Delta u \end{bmatrix} \quad (21)$$

$$\begin{bmatrix} y \\ z \\ w \end{bmatrix} = \begin{bmatrix} y \\ z \\ w \end{bmatrix} + step_D \begin{bmatrix} \Delta y \\ \Delta z \\ \Delta w \end{bmatrix} \quad (22)$$

where $step_P$ and $step_D$ are the step length in the primal and dual space, respectively.

$$step_P = 0.9995 \min \left\{ \min_i \left(\frac{-l_i}{\Delta l_i} : \Delta l_i < 0; \frac{-u_i}{\Delta u_i} : \Delta u_i < 0 \right), 1 \right\} \quad (23)$$

$$step_D = 0.9995 \min \left\{ \min_i \left(\frac{-z_i}{\Delta z_i} : \Delta z_i < 0; \frac{-w_i}{\Delta w_i} : \Delta w_i > 0 \right), 1 \right\} \quad i = 1, 2, \cdots, r \quad (24)$$

3 Computational Implementation

The size of the test systems used to evaluate the performance of the proposed formulation are listed in Table 1. The programming for solving is under Matlab 6.5 environment.

Table 1 Test system size and functional inequality constraints

System	Number of buses/lines	Constraints (V_i^2, P_{ij})	Constraints (L_i)
IEEE 4	4/4	4(3,1)	2
IEEE 14	14/20	16(13,3)	11
IEEE 30	30/41	35(29, 6)	24
IEEE 57	57/78	64(56,8)	53
IEEE118	118/179	127(117,10)	102

One step in solving the model is to initialize the related data of IPM. We set the iteration count $k = 0$, its maximum $K_{\max} = 50$, the centering parameter $\sigma = 0.1$ and tolerance $\varepsilon = 10^{-6}$. Other variables are chosen with $[z > 0, w < 0, y = 0]^T$ and $[l, u]^T \geq 0$.

The primal variables x should also be set as proper values. In this study, the real and imaginary parts of all voltages are respectively set as $e_i = 1$ and $f_i = 0$, and active power of generators and reactive output of reactive sources as the mean of their upper and lower limits, $x_i^{(0)} = (\overline{g}_i + \underline{g}_i)/2$.

During the programming process, the derivation of formula is an important job. For instance, in section 2, the term $\nabla^2 h(x)y$ in the correction equation (18) is

$$\nabla^2 h(x)y = Jacobian[\nabla h(x)y] \tag{25}$$

and the element at the *i-th* row and the *j-th* column is

$$\left[\nabla^2 h(x)y\right]_{ij} = \sum_{k=1}^{n_{eq}} \{y_k [\nabla^2 h_k(x)]_{ij}\} \tag{26}$$

where $\nabla^2 h_k(x)$ denotes the Hessian matrice of the elements in the *k-th* column of $h(x)$, n_{eq} is the number of equality constraints. (The proof can be seen from the appendix).

Considering that Matlab does well in vector operation, we need to transform the original optimal power flow model into vectors. For example, in our program the power mismatches at all buses

$$\begin{aligned} dertaP &= [\Delta P_1, \Delta P_2, \cdots, \Delta P_n]^T \\ dertaQ &= [\Delta Q_1, \Delta Q_2, \cdots, \Delta Q_n]^T \end{aligned} \tag{27}$$

are expressed as:

$$\begin{aligned} dertaP &= (PG - PD) - (e.*Te + f.*Tf) \\ dertaQ &= (QR - QD) - (f.*Te - e.*Tf) \end{aligned} \tag{28}$$

where

$$\begin{aligned} PG &= [P_{G1}, P_{G2}, \cdots, P_{Gn}]^T \\ PD &= [P_{D1}, P_{D2}, \cdots, P_{Dn}]^T \end{aligned} \tag{29}$$

$$\begin{aligned} QR &= [P_{R1}, P_{R2}, \cdots, P_{Rn}]^T \\ QD &= [Q_{D1}, Q_{D2}, \cdots, Q_{Dn}]^T \end{aligned} \tag{30}$$

$$\begin{aligned} e &= [e_1, e_2, \cdots, e_n]^T \\ f &= [f_1, f_2, \cdots, f_n]^T \end{aligned} \tag{31}$$

$$\begin{aligned} Te &= G*e - B*f \\ Tf &= G*f + B*e \end{aligned} \tag{32}$$

G and B are the real and imaginary part of the nodal admittance matrix, respectively.

Fig. 1 shows the solving process of our model, where the complementary gap

$$Gap \equiv \sum_{i=1}^{r} (l_i z_i - u_i w_i) \tag{33}$$

And the perturbed factor

$$\mu \equiv \sigma \cdot Gap / 2r \tag{34}$$

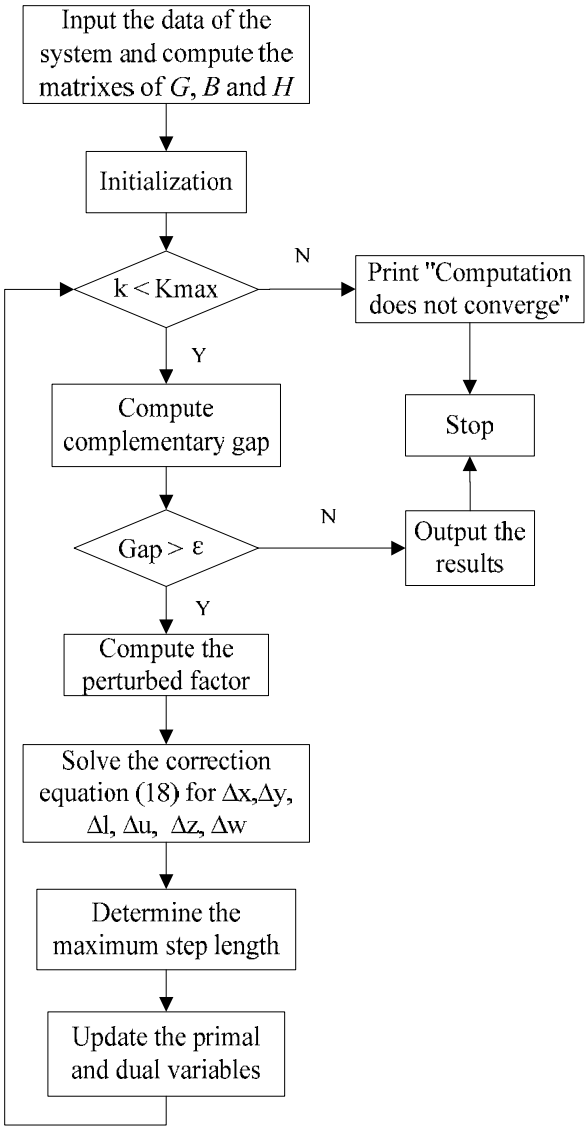

Fig. 1 The flowchart of solving our model

4 Test Results and Analysis

4.1 Case Study

Table 1 shows the test results for the system of IEEE 4, where $\overline{L}$ can be set by the system operators according to the practical operation to guarantee adequate voltage stability margin for the system. $L_{\max}$ is the maximum one among all the L indexes evaluated at load buses and the bus corresponding to $L_{\max}$ is the easiest one to lose voltage stability. $\sum P_G$ denotes the total output of active power of generators. F_{cost} is the total fuel cost of thermal plants. × denotes that no optimal solution is found.

Table 2 Test results for IEEE4 system

$\overline{L}$	$L_{\max}$	F_{cost} (\$/MWh)	$\sum P_G$ (pu)
1	0.4051	775.3974	1.6565
0.6	0.4051	775.3974	1.6565
0.4045	0.4045	775.9334	1.6565
0.4040	0.4040	776.3830	1.6565
0.4035	0.4035	776.8990	1.6566
0.403	0.403	777.5033	1.6567
0.4025	0.4025	778.2360	1.6568
0.402	0.402	779.1803	1.6571
0.4015	0.4015	780.5939	1.6574
0.401	×	×	×

To observe how the voltage stability constraints (L constraints) influence the fuel cost and system operation, we decrease $\overline{L}$ step by step to enhance the voltage security level of the system. In Table1, when $\overline{L}$ changes between 1 to 0.4051, L constraints do not take effect, so the fuel cost and P_G keep the same as the ones obtained when $\overline{L}=1$.

When $\overline{L}$ is lower than 0.4051, for example 0.4045, L constraints take effect and the maximum of L_i depends on $\overline{L}$. At the same time, the fuel cost and $\sum P_G$ rise with the decrease of $\overline{L}$. When $\overline{L}$ decreases to a certain value (0.4014 for this system), there is no optimal solution for the problem. This demonstrates that the voltage stability margin of a power system has a maximum value, and it can not be elevated without any limit.

For other test systems, Fig. 2, 3, 4 and 5 give the simulation results, where $\overline{L}$ is represented by *Lu*.

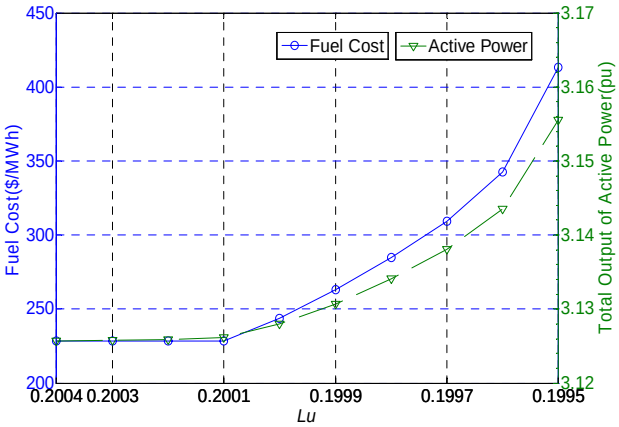

Fig. 2 Test results for IEEE14 system

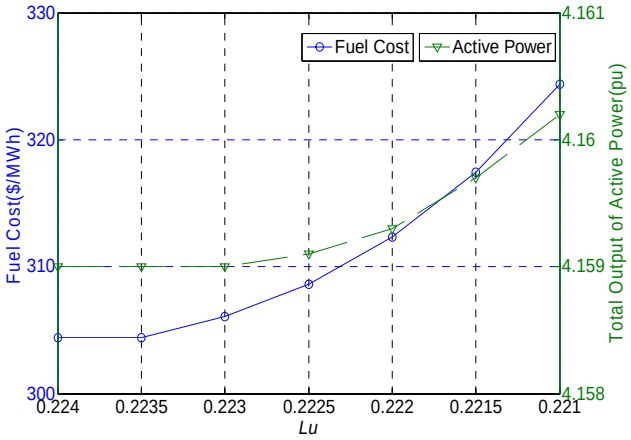

Fig. 3 Test results for IEEE30 system

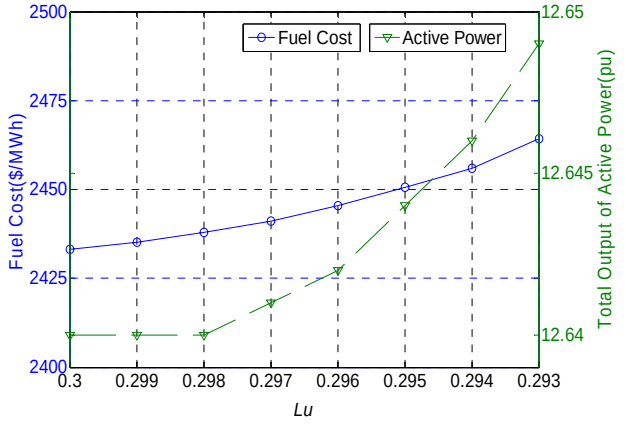

Fig. 4 Test results for IEEE57 system

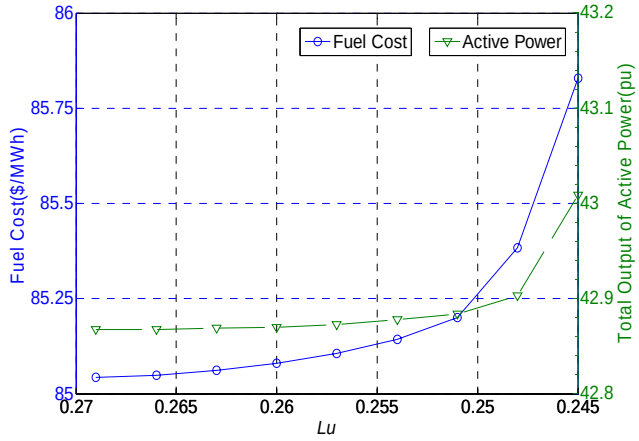

Fig. 5 Test results for IEEE118 system

By comparison of the above simulation results, some conclusions could be obtained as follows:

(1) If voltage stability constraints take effect, the total output of active power of generators and fuel costs will increase as $\overline{L}$ decreases. This shows the higher the system demands on voltage security, the more the fuel cost will be and the worse the economy will get.

(2) If voltage stability constraints take no effect, the incorporation of these constraints will not strengthen the system security and do no harm to the economy.

(3) The objective function value of our model with $\overline{L}=1$ is the same with that of the conventional OPF.

(4) The range that L constraints have an impact on the system is limited, which is much smaller than that in [25]. This is the main difference between using the initial form and simplified form of L index as voltage stability constraints. Obviously, this also verifies that the regulation ability of the system is affected by incorporation of these constraints.

(5) The L constraints have more effective influence on the improvement of the system stability at higher loading conditions.

Fig. 6 shows the fuel cost of our model (denoted by L-OPF in this figure) with effective L constraints is greater than that of the conventional OPF. In this case, the cost of OPF for all test systems is 100%. Lu is set as 0.4015, 0.1996, 0.221, 0.293 and 0.245 for the test systems of 4, 14, 30, 57 and 118 buses, respectively.

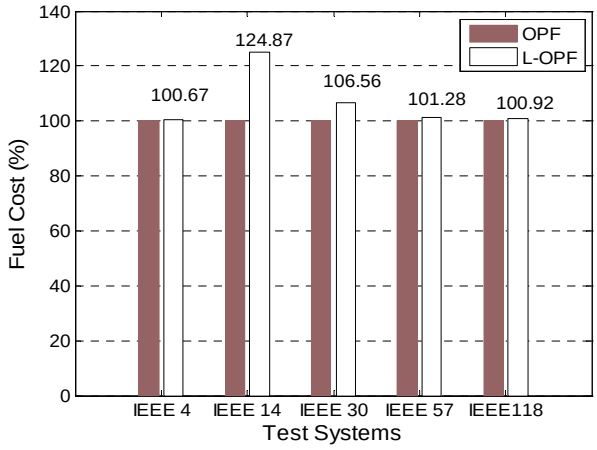

Fig. 6 The fuel cost of OPF and L-OPF

4.2 Performance of the Primal-Dual IPM

The complementary gap is a very important measure to judge the optimality of solutions and its change reflects the characteristic of the IPM. Fig. (7-11)

respectively show how it reduces with iterations for the above five test systems with $\overline{L}=1$ and other critical values, where $\overline{L}$ is denoted by *Lu*.

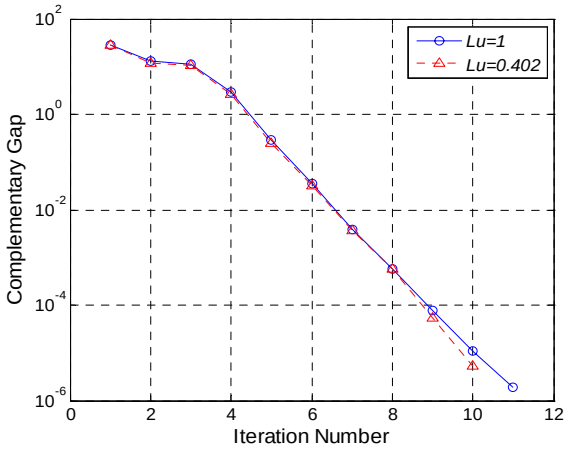

Fig. 7 Complementary gap with iterations for IEEE4 system

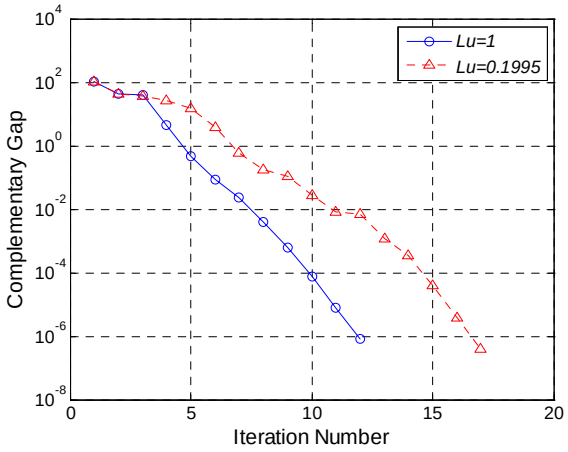

Fig. 8 Complementary gap with iterations for IEEE14 system

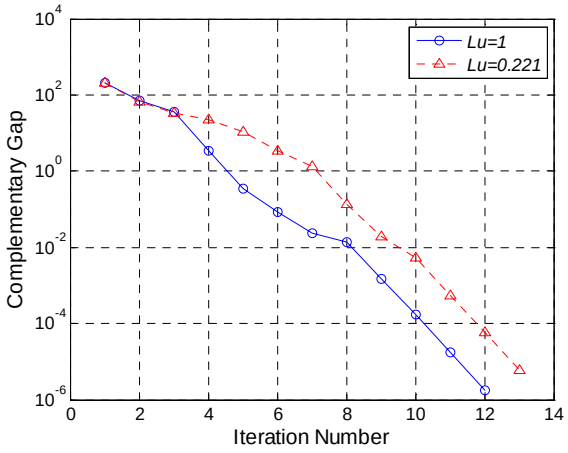

Fig. 9 Complementary gap with iterations for IEEE30 system

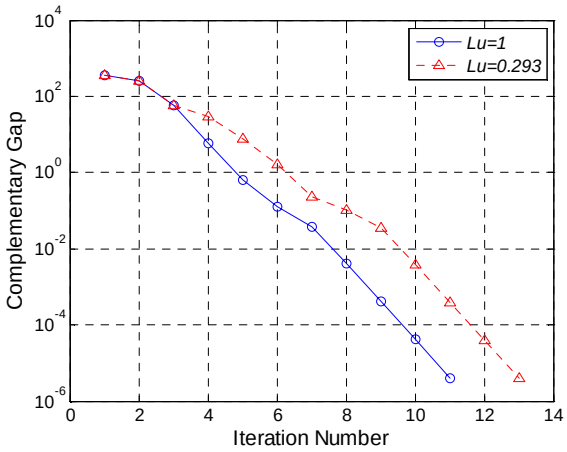

Fig. 10 Complementary gap with iterations for IEEE57 system

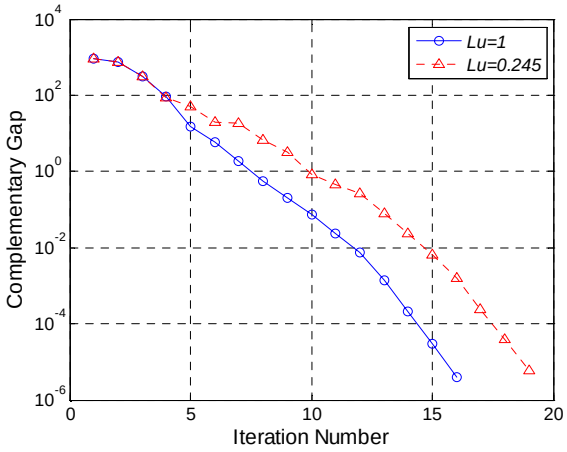

Fig. 11 Complementary gap with iterations for IEEE118 system

From the above figures, it can be seen that:

(1) For the same system, the convergence curves of our model have no significant difference when $\overline{L}$ is set as 1 and other critical values.

(2) The selection of $\overline{L}$ has no big influence on iteration numbers of this algorithm;

(3) The complementary gaps decrease to zero monotonically and rapidly;

(4) The iteration number changes between 9 and 19 for all test systems.

Therefore, the perturbed-KKT-condition based primal-dual IPM shows robustness and good convergence. It is suitable for solving optimal power flow problems with voltage stability constraints.

5 Conclusion

The operation of power systems has been significantly affected by the deregulation process. Nowadays, increased load demand and the need to operate the system based mainly on economic considerations have led to many concerns regarding the secure operation of power systems. Hence, there is a need for incorporating voltage stability into the OPF that can guarantee system stability within the context of a market operating environment.

In this paper, a novel OPF formulation that can consider voltage stability constraints has been proposed. The initial form of L-index is used to indicate the voltage stability margin. The solution of this model can maintain the demanded voltage security level in the most economical way. Simulations have shown that the enhancement of voltage stability of the systems will increase the total operation cost. The incorporation of L constraints affects the regulation ability of the system and the effective range of these constraints is limited. Furthermore, the primal-dual IPM is proposed as the computation approach, which is proved to be efficient and has good convergence by the simulation results.

References:

[1] J. Carpentier, Contribution to the economic dispatch problem, *Bull. Sac. France Elect.*, Vol. 8, 1962, pp. 431-437.

[2] M. Geidl, G. Andersson, Optimal power flow of multiple energy carriers, *IEEE Trans. Power System*, Vol. 22, No. 1, 2007, pp. 145-155.

[3] Abdel-Moamen M.A., Padhy N.P., Optimal power flow incorporating FACTS devices-bibliography and survey, *Proc. of IEEE/PES Transm. and Distrib. Conference and Exposition*, Vol.2, 2003, pp. 669-676.

[4] A. Kurita, T. Sakurai, The power system failure on July 23, 1987 in Tokyo, *Proc. 27th IEEE Conf. on Decision and Control*, Vol.3, 1988, pp. 2093-2097.

[5] Y. Mansour, *Voltage Stability of Power Systems: Concepts, Analytical Tools and Industry Experience*, IEEE Press, 1990.

[6] G. Carpinelli, D. Lauria, P. Varilone, Voltage stability analysis in unbalanced power systems by optimal power flow, *IEE Proc. – Gener., Transm. Distrib.*, Vol. 153, No. 3, 2006, pp. 261-268.

[7] C. Aumuller, T. K. Saha, Analysis and assessment of large scale power system voltage stability by a novel sensitivity based method, *Proc. of IEEE/PES Summer Meeting*, Vol. 3, 2002, pp. 1621-1626.

[8] Y. Mansour, Ed. *Suggested Techniques for Voltage Stability Analysis*, IEEE Press, 1993.

[9] GIGRE Task Force 38-02-11, Indices predicting voltage collapse including dynamic phenomenon, *CIGRE technical report*, 1994.

[10] A. Berizzi, P. Finazzi, D. Dosi, et al, First and second order methods for voltage collapse assessment and security enhancement, *IEEE Trans. Power System*, Vol. 13, No. 2, 1998, pp. 543-551.

[11] A. Berizzi, P. Bresesti, P. Marannino, M. Montagna, S. Corsi, and G. Piccini, Security enhancement aspects in the reactive-voltage control, *IEEE Stockholm Power Tech*, Vol. Power Systems, 1995, pp. 674–679.

[12] T. Esaka, Y. Kataoka, T. Ohtaka, S. Iwamoto, Voltage stability preventive and emergency preventive control using VIPIt sensitivities, *Proc. of IEEE/PES Power Systems Conference and Exposition*, Vol.1, 2004, pp. 509-516.

[13] N. Yorino, T. Usui, H. Sasaki, J. Kubokawa, M. Kitagawa, and K. Fujioka, An effective monitoring of power system voltage stability by means of voltage stability indices, *Trans IEE of Japan*, Vol. 111-B, No. 3, 1991, pp. 267–276.

[14] M. Nanba, Y. Huang, T. Kai, and S. Iwamoto, Studies on VIPI based control methods for improving voltage stability, *Proc. PSCC*, Vol. 2, 1996, pp. 651–657.

[15] Cai Li-Jun, Erlich Istvan, Power system static voltage stability analysis considering all active and reactive power controls - singular value approach, *Proc. of IEEE Power Tech.*, 2007, pp. 367-373.

[16] Y. Wang, L. C. P. Da Silva, W. Xu, Y. Zhang, Analysis of ill-conditioned power-flow problems using voltage stability methodology, *IEE Proc. – Gener., Transm. Distrib.*, Vol.148, No. 5, 2001, pp. 384-390.

[17] R. A. Schlueter, S. Z. Liu, K. B. Kilani, Justification of the voltage stability security assessment and diagnostic procedure using a bifurcation subsystem method, *IEEE Trans. Power System*, Vol. 15, No. 3, 2000, pp. 1105-1111.

[18] K. A. Folly, J. K. Mukusuka, Voltage stability of AC-DC interconnections as affected by AC line length, *Proc. of IEEE Power Tech.*, 2007, pp.178-183.

[19] S. Greene, I. Dobson, and F.L. Alvarado, Sensitivity of the loading margin to voltage collapse with respect to arbitrary parameters, *IEEE Trans. on Power Systems*, Vol. 12, No. 1, 1997, pp. 262-272.

[20] I. A. Momoh and R. J. Koessler, et al., Challenges to optimal power flow, *IEEE Trans. Power Systems*, Vol. 12, No. 1, 1997, pp. 444-455.
[21] D. Gan, R. J. Thomas, and R. D. Zimmerman, Stability-Constrained Optimal Power Flow, *IEEE Trans. on Power Systems*, Vol.15, No. 2, 2000, pp. 535-540.
[22] W. Rosehart, C. Canizares, V. Quintana, Costs of voltage security in electricity markets, *Proc. of IEEE/PES Summer Meeting*, Vol. 4, 2000, pp. 2115-2120.
[23] K. Ramesh, F. Ali, Impact of VAR support on electricity pricing in voltage stability constrained OPF market model, *Proc. of IEEE/PES General Meeting*, 2007, pp. 1-6.
[24] Wu G.Y., Chung C.Y., Wong K.P., et al, Voltage stability constrained optimal dispatch in deregulated power systems, *IET Gener. Transm. Distrib.*, Vol. 1, No. 5, 2007, pp. 761–768.
[25] S. Kim, T.Y. Song, M.H. Jeong, et al, Development of voltage stability constrained optimal power flow (VSCOPF), *Proc. of IEEE/PES Summer Meeting*, Vol.3, 2001, pp. 1664-1669.
[26] P. Kessel, H. Glavitch, Estimating the voltage stability of a power system, *IEEE Trans. Power Delivery*, Vol. PWRD-1, No. 3, 1986, pp. 346-354.
[27] H. Wei, H. Sasaki, J. Kubokawa, et al, An interior point nonlinear programming for optimal power flow problems with a novel data structure, *IEEE Trans. Power System*, Vol. 13, No. 2, 1998, pp. 870-877.
[28] Karmarkar N, A new polynomial-time algorithm for linear programming, *Combinatarica*, Vol. 4, No. 4, 1984, pp. 373-395.
[29] H. Wei, H. Sasaki, J. Kubokawa, et al, Large scale hydrothermal optimal power flow problems based on interior point nonlinear programming, *IEEE Trans. Power System*, Vol. 15, No. 1, 2000, pp. 396- 403.

Appendix

To illustrate this clearly, we assume:

$$\nabla h(x) = \begin{bmatrix} \frac{\partial h_1}{\partial x_1} & \frac{\partial h_2}{\partial x_1} \\ \frac{\partial h_1}{\partial x_2} & \frac{\partial h_2}{\partial x_2} \end{bmatrix}, \; y = \begin{bmatrix} y_1 \\ y_2 \end{bmatrix}$$

Then

$$Jacobian[\nabla h(x) y] = Jacobian \begin{bmatrix} y_1 \frac{\partial h_1}{\partial x_1} + y_2 \frac{\partial h_2}{\partial x_1} \\ y_1 \frac{\partial h_1}{\partial x_2} + y_2 \frac{\partial h_2}{\partial x_2} \end{bmatrix}$$

$$= \begin{bmatrix} \frac{y_1 \frac{\partial h_1}{\partial x_1} + y_2 \frac{\partial h_2}{\partial x_1}}{\partial x_1} & \frac{y_1 \frac{\partial h_1}{\partial x_1} + y_2 \frac{\partial h_2}{\partial x_1}}{\partial x_2} \\ \frac{y_1 \frac{\partial h_1}{\partial x_2} + y_2 \frac{\partial h_2}{\partial x_2}}{\partial x_1} & \frac{y_1 \frac{\partial h_1}{\partial x_2} + y_2 \frac{\partial h_2}{\partial x_2}}{\partial x_2} \end{bmatrix}$$

$$= \begin{bmatrix} y_1 \frac{\partial h_1}{\partial x_1 \partial x_1} + y_2 \frac{\partial h_2}{\partial x_1 \partial x_1} & y_1 \frac{\partial h_1}{\partial x_1 \partial x_2} + y_2 \frac{\partial h_2}{\partial x_1 \partial x_2} \\ y_1 \frac{\partial h_1}{\partial x_2 \partial x_1} + y_2 \frac{\partial h_2}{\partial x_2 \partial x_1} & y_1 \frac{\partial h_1}{\partial x_2 \partial x_2} + y_2 \frac{\partial h_2}{\partial x_2 \partial x_2} \end{bmatrix}$$

So the *ij-th* element of $\nabla^2 h(x) y$ is

$$\left[\nabla^2 h(x) y\right]_{ij} = \sum_{k=1}^{n_{eq}} \{y_k [\nabla^2 h_k(x)]_{ij}\}$$